

PAN: Pulse Ansatz on NISQ Machines

Zhiding Liang^{*1} Jinglei Cheng^{†1} Hang Ren[‡] Hanrui Wang[§] Fei Hua[¶] Yongshan Ding^{||}
Fred Chong^{**}, Song Han[§] Yiyu Shi^{*} Xuehai Qian[†]

^{*}University of Notre Dame [†]Purdue University [‡]University of California, Berkeley

[§]Massachusetts Institute of Technology [¶]University of Rutgers

^{||}Yale University ^{**}University of Chicago

¹These authors contributed to the work equally and should be regarded as co-first authors.

Corresponding authors: zliang5@nd.edu, cheng636@purdue.edu

Abstract—Variational quantum algorithms (VQAs) have demonstrated great potentials in the NISQ era. In the workflow of VQA, the parameters of ansatz are iteratively updated to approximate the desired quantum states. We have seen various efforts to draft better ansatz with less gates. Some works consider the physical meaning of the underlying circuits, while others adopt the ideas of neural architecture search (NAS) for ansatz generator. However, these designs do not exploit full advantages of VQA. Because most techniques are targeting gate ansatz, and the parameters are usually rotation angles of the gates. In quantum computers, the gate ansatz will eventually be transformed into control signals such as microwave pulses on transmons. And the control pulses need elaborate calibration to minimize the errors such as over-rotation and under-rotation. In the case of VQAs, this procedure will introduce redundancy, but the variational properties of VQAs can naturally handle problems of over-rotation and under-rotation by updating the amplitude and frequency parameters. Therefore, we propose PAN, a native-pulse ansatz generator framework for VQAs. We generate native-pulse ansatz with trainable parameters for amplitudes and frequencies. In our proposed PAN, we are tuning parametric pulses, which are natively supported on NISQ computers. Considering that parameter-shift rules do not hold for native-pulse ansatz, we need to deploy non-gradient optimizers. To constrain the number of parameters sent to the optimizer, we adopt a progressive way to generate our native-pulse ansatz. Experiments are conducted on both simulators and quantum devices to validate our methods. When adopted on NISQ machines, PAN obtained improved the performance with decreased latency by an average of 86%. PAN is able to achieve 99.336% and 96.482% accuracy for VQE tasks on H_2 and HeH^+ respectively, even with considerable noises in NISQ machines.

I. INTRODUCTION

Operating on the principles of quantum mechanics, quantum computers have the potential to solve problems that are intractable on classical digital computers [4], [12], [44]. As the hardware technologies and quantum algorithms advance rapidly, today’s quantum computers begin to demonstrate their advantage in solving problems of non-trivial size in areas such as quantum chemistry [9]. In 2019, Google claimed to have achieved quantum supremacy with the task of random circuit sampling with a 53-qubit quantum computer [8]. IBM launched its 127-qubit quantum computer at the end of 2021, together with a roadmap for quantum processors with more than ~ 1000 qubits in the coming years [1]. In the current NISQ era, however, emerging quantum devices are still prone to errors (with noisy gate operations, measurements) and sensitive to decoherence [26], [41], [79].

In NISQ computers, qubits are scarce and not perfectly isolated with the environments, and operations (such as quantum gates and measurements) are often noisy. These quantum devices do not yet meet the requirements for error correction such as surface codes [22], [23], [27], [40], [68] due to the limited qubit count and low gate fidelity. Because of the hardware noises, current quantum computers can only execute small-scale circuits before running into irreversible errors, making some practical algorithms infeasible. However, with intricately designed noise-resilient algorithms, we can still expect to achieve quantum supremacy in areas such as quantum chemistry [16], [47], [67], [72] much sooner than other applications like database search [37] and integer factorization [65].

Variational quantum algorithms (VQAs) [7], [17], [38], [51], [66], [76] have shown great noise resilience, and are often considered as hybrid algorithms, where some steps are performed on a quantum device and others on a classical computer. Variational quantum eigensolver (VQE) [43], [50], [74] is one of the most promising candidates in the variational computing paradigm. The objective of a VQE is to estimate the ground state energy of a targeting quantum system by iteratively evaluating and updating a parametrized quantum circuit. With VQE, we are able to solve electronic structure problem on quantum computers. Quantum approximate optimization algorithm (QAOA) [38] and quantum neural network (QNN) [3] are also members of VQA. QAOA attempts to solve combinatorial optimization problems including max-cut problem. And QNN has exhibited capabilities to represent complex data [39], [63]. These algorithms are among the most promising examples of NISQ algorithms since the number of required quantum gates remain moderate.

Exposing Native Pulse-Level Controls. The majority of existing quantum computers do not provide application programming interfaces (APIs) for analog control of qubits. As a result, nearly all compilers implement a gate-based workflow [48], [71], in which quantum algorithms are synthesized, compiled, and finally executed on quantum computers. In the first place, the construction of quantum algorithms will result in circuits that use gates as their elements. Most of the time, these circuits are not compatible with the underlying topology of quantum hardware. In order to map and decompose the circuits onto the physical qubits, a compiler is required. During the compilation process, SWAP gates are inserted so that the

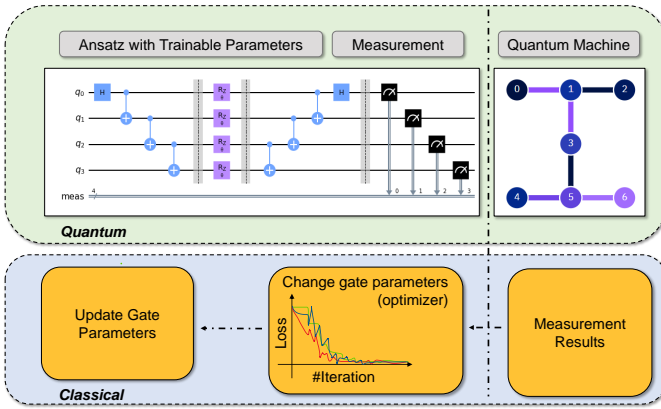


Fig. 1. A traditional procedure for gate-based quantum variational algorithms. During each iteration, gradient information is used to update the ansatz’s parameters. Gradients are “calculated” using finite difference techniques or shit-parameter rules.

topology restrictions can be satisfied. At the same time, circuits are decomposed into single-qubit and two-qubit native gates so that they can be processed by the quantum hardware. Then the circuits will be dispatched to quantum backends, where they are “translated” into control signals on physical qubits such as transmons [61], trapped ions [13] and photons [45]. For superconducting quantum computers, the control signals are composed of microwave pulses [6].

Intuitively, there is potentially more possibility for improvement if the gate circuits are further decomposed and tuned at the pulse level. Once the circuits have been compiled into pulses rather than gates, we will be able to remove the abstraction layer of native gates. As a result, the challenge now is to figure out how to produce pulses for quantum algorithms in an effective manner. Existent techniques like quantum optimal control (QOC) [19], [54], [78] can be used to optimize the generation of control pulses. QOC devises and implements the shapes of external controls on qubits to accomplish given tasks. As indicated in [64], QOC can handle quantum circuits of moderate size, but the scalability might be the issue. Despite various efforts [18], [46] to optimize QOC and reduce its overhead, it is still computationally expensive. Also, we need to consider the high-noise feature of NISQ devices, on which it is preferred to have a fixed set of allowed operations or gates. This small group of operations or gates can be carefully calibrated to reach the maximum fidelity [6]. The calibrations are conducted regularly to enforce high accuracy. Therefore, it is generally hard to take advantage of quantum pulses with NISQ machines. The reasons are the high noise of quantum hardware and the exceptional overhead of the pulse generator.

Why Pulses for VQAs? Situations differ slightly in the case of VQAs due to its variational characteristics. Specifically, during the “training” process, the parametric circuits of VQAs are updated. It is now unimportant whether the gates are accurately implemented on quantum hardware as long as the parametric circuits can reach desired states. Specifically, instead of using

gate-level compilation or QOC, we can implement quantum algorithms at the “native-pulse level”. At the native-pulse level, we can directly manipulate the native pulses that are supported by the hardware. This paradigm shift grants finer-grained control and thus making it possible for better performance, scalability, and robustness. Recent work [32] has shed light on the feasibility and potential for such a paradigm shift. However, the research on pulse level optimization is still in its infancy. The capability of quantum pulses has not been fully explored, nor are they robust or scalable on NISQ machines. As summarized in Table I, many critical issues remain unsolved. Existing works, for instance, do not consider noise or system models of NISQ devices. Most of these pulses are therefore incompatible with NISQ machines.

To tackle these challenges, we propose PAN, a native-pulse ansatz generator for VQAs. PAN is the first to demonstrate the feasibility of native-pulse ansatz on NISQ machines. In PAN, we use native pulses to construct the variational part of the circuits, which is often referred to as ansatz. Instead of applying QOC, we directly train the pulses that are natively supported by the quantum processors. Compared with QOC, PAN has fewer parameters and can be easily deployed onto NISQ machines, while QOC with realistic system models will require huge computation resources. On the other side, PAN is superior to gate-based methods, since PAN drops the abstraction layer of native gates and induces less circuit latency. We provide results from IBM’s superconducting quantum computers [52], unlike previous work at the pulse level that was only evaluated on simulators.

Contributions. The goal of this paper is to construct native-pulse ansatz for VQAs and demonstrate in both simulator and NISQ machine. The major contributions of PAN include:

- **Native-pulse ansatz.** Our native-pulse ansatz is derived from “native” pulses extracted from quantum backends. In this manner, we ensure that pulse ansatz is compatible with quantum hardware.
- **Progressive learning.** In PAN, a non-gradient optimizer is employed. We provide a progressive way to “expand” our native-pulse ansatz in order to keep the total number of parameters sent to the optimizer to a moderate size. The newly appended pulses arrive with zero amplitudes at different phases of the progressive learning process. This prevents the appended pulses from abruptly changing the ansatz circuits’ overall unitaries.
- **Results from NISQ machines.** Experiments are carried out on simulators and NISQ machines. The results show that the native-pulse ansatz outperforms the gate ansatz for VQAs. We are able to reduce errors from qubit decoherence due to the short duration time of our native-pulse ansatz.
- **Exploration on frequency tuning.** We study the potential benefits of tuning the pulse frequencies on transmons so that the pulse learning paradigm can be enhanced. Experimental results show that frequencies could become extra degrees of freedom for the native-pulse ansatz.

Evaluation Highlights. Six NISQ machines are used in in

TABLE I
COMPARISON BETWEEN GATE-LEVEL APPROACHES, PULSE-LEVEL APPROACHES AND THE PROPOSED PAN

Method	Robustness		Parameters of Control		Applications		
	Noise-aware	System model	Amp.	Freq.	VQE	QAOA	QML
Gate-level (conventional)	✓	✓	✗	✗	✓	✓	✓
Pulse-level attempts [19], [54]	✗	✗	✓	✓	✓	✗	✗
PAN (Proposed)	✓	✓	✓	✓	✓	✓	✓

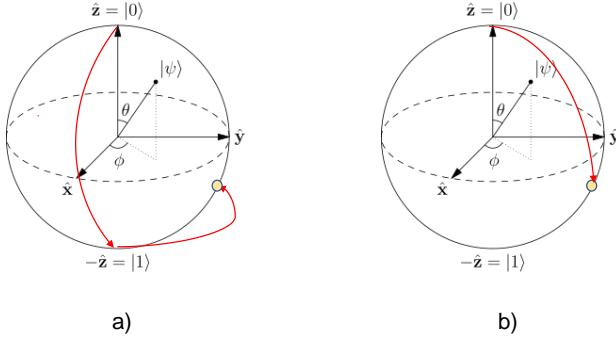


Fig. 2. Illustrations of the redundancy introduced by current gate-level compilation workflow. Pulse-level control does not require the transition to another basis before rotation. Path for searching target a) With gate-level approach. b) With pulse-level approach.

our studies to validate the proposed framework. We achieved a reduction of up to 97.3% in duration time and improved ansatz performance compared to baselines. In addition to the reduction in latency for ansatz, we attain an accuracy of 99.895% for a small electronic structure problem. The accuracy is achieved by a toy native-pulse ansatz produced by PAN.

II. BACKGROUND

A. Qubit and Quantum Gate.

In classical computing, the basic element to represent data is bit (0 or 1). Similarly, in quantum computing, the basic element to represent data is quantum bit (qubit). While classical bits are limited to the values 0 and 1, qubits can express linear combinations of two states that correspond to 0 or 1. The state of a qubit $|\psi\rangle$ can be described as a linear combination of the state 0 (i.e., $|0\rangle$) and state 1 (i.e., $|1\rangle$): $|\psi\rangle = \alpha|0\rangle + \beta|1\rangle$. α and β are the coefficients of state $|0\rangle$ and state $|1\rangle$. The probability that the qubit will be measured in the state $|0\rangle$ is $|\alpha|^2$ and the probability that it will be measured in the state $|1\rangle$ is $|\beta|^2$. Therefore, we have $\alpha^2 + \beta^2 = 1$. In analogy with classical computation, qubits are operated via quantum gates to perform a function. For instance, the X gate is used to transform the state of a qubit from $\alpha|0\rangle + \beta|1\rangle$ to $\beta|0\rangle + \alpha|1\rangle$. When the CNOT gate, which allows interactions between two qubits, is applied to the state $|10\rangle$, the result is state $|01\rangle$. Quantum gates are the building blocks of quantum circuits, which can use to manipulate the state of the qubits and utilized to implement a variety of quantum algorithms.

B. Variational Quantum Algorithms (VQAs)

The variational quantum eigensolver (VQE) is one of the most popular and promising VQAs for demonstrating quantum supremacy. VQE is employed primarily to solve the ground and low-excited states of quantum systems, but it also has important applications in quantum many-body physics, quantum chemistry, and other domains [43], [59], [70]. It calculates Hamiltonian ground state energy using the variational approach. Given a Hamiltonian H and a trial wavefunction $|\varphi\rangle$, the ground state energy E_0 is bounded by:

$$E_0 \leq \frac{\langle \psi | H | \psi \rangle}{\langle \psi | \psi \rangle} \quad (1)$$

The accuracy of the classical calculation method is restricted by the amount of computation required to model the exponentially growing Hamiltonian. VQE, on the other hand, can model complex wave functions in polynomial time. VQE has also been shown to be noise resistant in NISQ devices as a variational quantum algorithm [74]. The Quantum Approximate Optimization Algorithm (QAOA) is a variational quantum algorithm that solves combinatorial optimization problems with sub-optimal solutions [29], [38]. It is commonly believed that QAOA can establish quantum superiority in NISQ computers with shallow circuits. The ability to rapidly find the optimal variational parameters for general shallow quantum circuits is essential for demonstrating the potential quantum advantages of NISQ devices. Quantum neural network (QNN) is a model of quantum machine learning (QML) that use ansatz circuits to extract features from input data, followed by complex-valued linear transformations. QNN has great potentials for applications in QML [5], [11], quantum simulation and optimization [55].

C. Variational Quantum Circuit

Variational quantum circuits (VQC), also known as ansatz, enable the parameterization of quantum gates, hence facilitating the trainability of quantum circuits. VQC was initially proposed for quantum phase estimation, but additional research found that classical-quantum co-optimization methodologies can also be leveraged for other applications. Variational quantum circuits are fundamental VQA components. As illustrated in Figure 1, VQC is in the quantum part of the method. The classical computer will assign new parameters to the VQCs and collect the outputs of the quantum machines. Designing ansatz is essential for VQAs since different designs have a substantial effect on VQA performance. In the field of

quantum chemistry, numerous ansatz with physical insights, such as UCCSD [10], are developed. In the subject of quantum machine learning, the optimal ansatz is determined using neural architecture search techniques [75].

D. Quantum Optimal Control

Assuming a closed quantum system for quantum optimal control, the system's Hamiltonian is provided by

$$H(t) = H_0 + \sum_{j=1} u_j(t)H(j) \quad (2)$$

where H_0 is the drive Hamiltonian, $H(j)$ is the control Hamiltonian, and u_j is time-dependent amplitude signal. Schrödinger's equation governs the system's dynamics:

$$\frac{d}{dt}|\psi\rangle = -iH(t)|\psi\rangle \quad (3)$$

where ψ_0 denotes the system's state at time $t = 0$. Quantum optimum control (QOC) can be used to calculate $u_j(t)$ in order to adjust the Hamiltonian and drive state-state transfer. Using QOC, for instance, we can transform a random state into a desired state. The QOC generator will create pulse signals with pulse simulators like Qutip [42] or Qiskit [52]. Typically, a cost function is specified as the pulse's fidelity, which can be estimated as the difference between the simulated unitary matrix and the desired unitary matrix. Algorithms like GRAPE [24] and CRAB [15] can be applied to calculate the control signals.

E. Quantum Pulse Learning

Another method of generating pulses is to parameterize the quantum pulse and then optimize the parameters. We refer to such process as quantum pulse learning. For quantum computers with transmon as qubits, the Hamiltonian can be described as follows to understand the trainable components of control pulses:

$$H = \sum_{i=0}^1 (U_i(t) + D_i(t))\sigma_i^X + \sum_{i=0}^1 2\pi\nu_i(1 - \sigma_i^Z)/2 + \omega_B a_B a_B^\dagger + \sum_{i=0}^1 g_i \sigma_i^X (a_B + a_B^\dagger) \quad (4)$$

$D_i(t)$ and $U_i(t)$ are two major terms that govern the pulse learning, they are derived in Equation 5. They are obtained by mixing local oscillator with control signals. σ_X , σ_Y , and σ_Z are Pauli operators. ν_i is the estimated frequency of qubits in the qubit i , g_i is the coupling strength between qubits, ω_B is the frequency of control buses, a_B and a_B^\dagger are the ladder operator for control buses.

$$\begin{aligned} D_i(t) &= \text{Re}(d_i(t)e^{i\omega_{a_i}t}) \\ U_i(t) &= \text{Re}[u_i(t)e^{i(\omega_{a_i} - \omega_{a_j})t}] \end{aligned} \quad (5)$$

where $d_i(t)$ and $u_i(t)$ are the signals of qubit i on drive channel and control channel. Since pulse learning adjust $d_i(t)$ and $u_i(t)$, $D_i(t)$ and $U_i(t)$ are changed accordingly. Consequently,

the drive Hamiltonian is also updated [49]. Thus, we are able to govern the quantum system using control signals. Numerous publications have examined how to benefit from such scheme. For example, Ctrl-VQE [54] propose to optimize pulse shapes for the state preparation. Since these approaches do not target real NISQ machines, they are subject to the vulnerabilities outlined in Section I.

F. Current NISQ machines

Several prospective material systems are being researched in order to build and implement qubits and quantum gates. Material systems include trapped ions [58], optical lattices [36], nuclear magnetic resonance (NMR) [73], diamond [56], and superconducting circuits [20]. Superconducting circuit is one of the most leading candidate to build a quantum computer of realizing the computations beyond the reach of classical computer. In superconducting transmon system, Quantum gates are implemented by driving the target qubit through the microwave in the pulse level [6]. For example, the Rx and Ry rotations can be implemented by sending microwave voltage signals. However due to the imperfect implementations, efficiently and precisely microwave pulse control remains as an open question which also provide more optimization opportunity for design spaces.

III. MOTIVATION

A. Deficiencies of Gate-level Compiler

Figure 4 illustrates the execution of a quantum computing program from high-level programming to the compiler on quantum machines. In the case of variational quantum algorithms, the ansatz consists of parametric gates if the conventional compilation workflow is utilized. Redundancy will be introduced by the existing implementation of rotation gates on quantum hardware. For example, we want the qubit to evolve to the point on the Bloch sphere as indicated in Figure 2. It will first complete the basis transformation, then a phase shift, followed by a second basis transformation to reach the point on qubits. The example demonstrates the redundancy when quantum circuits are compiled into native gates. We propose to bypass the abstract layer of native gates and use native pulses directly as the parametric elements in the ansatz.

B. Drawbacks of Optimal Control Pulses

In addition, attempts have been made to optimize the quantum pulse generator. For example, [33], [78] proposes using quantum optimal control (QOC) to generate pulses for given unitaries. The applications of quantum pulses are severely constrained by the excessive cost of pulse generators and the complexity of NISQ devices' system models. In addition, the gradient-based approach with back propagation cannot be used, because gradients for pulses are not accessible on the backend of NISQ machines. As a result, the PAN must deal with non-gradient optimizers. Non-gradient optimizers, on the other hand, have a high computational cost and a substantial degree of uncertainty when dealing with high-dimensional spatial parameters. This is because a large number of samples

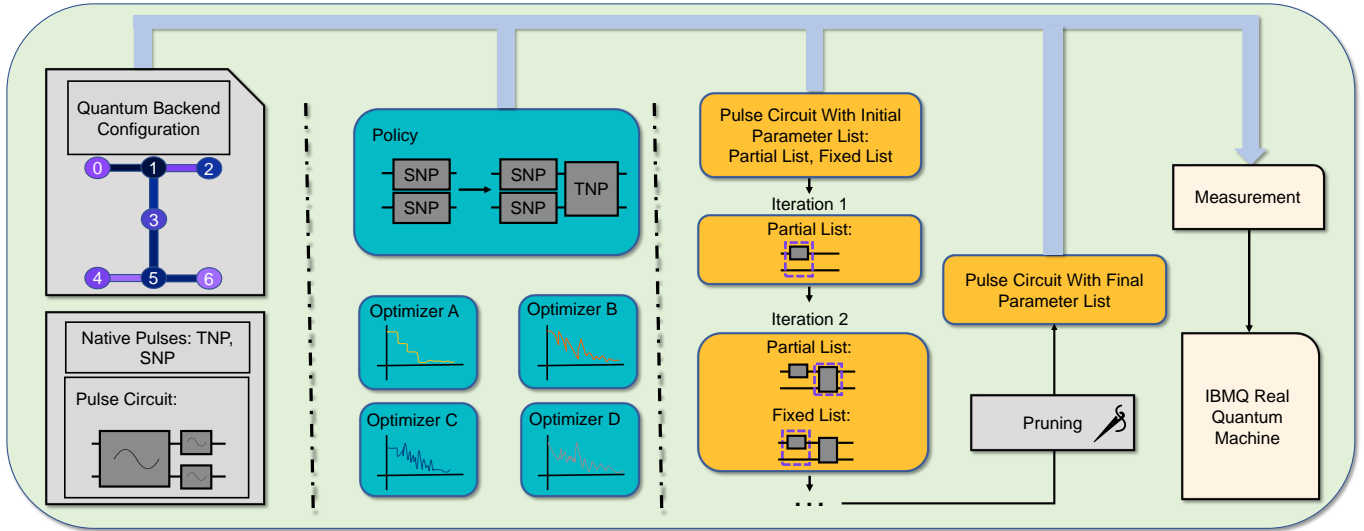


Fig. 3. The overview of design and implementation of PAN. First, a pulse ansatz using single-qubit native pulses (SNP) and two-qubit native pulses (TNP) is introduced. Then the ansatz is trained and updated in a progressive way, where parameters are divided into a “partial” list and a fixed list. Only parameters inside the “partial” list will be updated. Furthermore, a pulse pruning method is proposed to remove redundant pulses. Finally, the pulses are executed on NISQ machines.

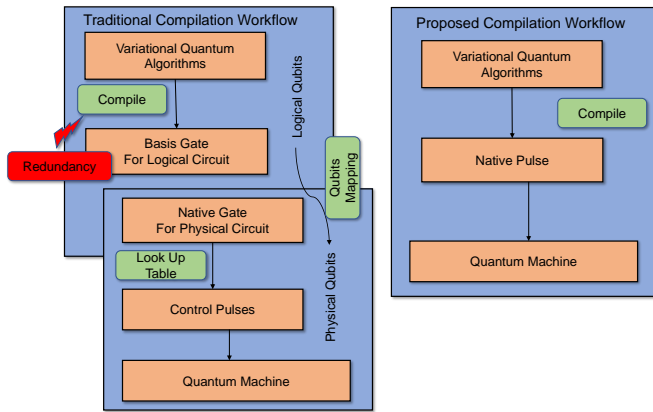


Fig. 4. Comparison between compilation process for gate level and pulse level. Gate-level workflow consists of several layers and introduce redundancy, pulse-level workflow consists few layers that can gain benefits on latency.

must be frequently pre-set or executed throughout the processing procedure. Because pulses contain more parameters than gates, it is inefficient to train the whole pulse ansatz with a non-gradient optimizer.

C. Potentials of Pulse Ansatz

As the illustration in Figure 2, if we can directly control pulses, we can eliminate some degree of redundancy. This allows us to reduce the program’s overall latency. Specifically, decoherence errors will decrease. The absence of calibration may result in inaccuracies. However, our focus is on VQAs, whose circuits are dynamic. Through parameter tuning, the pulse ansatz can correct for errors such as under-rotation and over-rotation. In addition to the amplitudes of native pulses, the frequency of qubit channels can be adjusted. In conclusion,

pulse ansatz offers greater degrees of freedom, enabling us to achieve the desired states with substantially shorter pulse lengths.

IV. OVERVIEW OF PAN FRAMEWORK

In the proposed scheme for native-pulse ansatz, the pulse parameters are given by the drive Hamiltonian in Equation 4. During real quantum computer evaluations, however, gradients cannot always be obtained. We use a gradient-free optimizer to train the pulse parameters in the ansatz. In high-dimensional space, however, none of the optimizers can gain an advantage over a random parameter search. Therefore, we offer a progressive method for generating our native-pulse ansatz. This structure of progressive learning assures that the optimizer’s parameter dimensions during training do not exceed the capacity. And the optimized machine-in-loop training method makes the framework noise-resilient. Such a system is well-suited for pulse-level learning algorithms to address the noise issue in NISQ machines while minimizing the number of parameters handled by the optimizer.

We illustrate the workflow of the proposed framework PAN in Figure 3. First of all, the configurations of the NISQ computers must be extracted. The configurations include information regarding qubit frequencies and the mapping between native gates and native pulses. Once we have the frequencies and pulses supported by the backend, we can begin to develop our native-pulse approach. The native-pulse ansatz is constructed from the extracted pulses’ structures. We are able to confirm that the extracted pulses are compatible with the quantum hardware, and we may adjust the amplitudes to achieve a variety of functionalities.

After obtaining the candidates for native pulses, we can progressively construct our native-pulse ansatz. Similar to the

hardware-efficient ansatz, single-qubit gates are placed for each qubit and two-qubit gates are applied to all potential connections. The single-qubit pulse may consist of pulses retrieved from the Hadamard gate or the Rx gate. And the two-qubit pulses are derived from the CX gate or CR gate pulses. In our framework, pulses from CR gates are preferred because they are the simplest two-qubit pulses that enable the entanglement of two qubits. Thus, we now have two distinct types of layers. One consists of single-qubit native pulses on all qubits, whereas the other consists of two-qubit native pulses on all connections. The two types of layers are successively inserted during the training process to further explore the Hilbert space. To train the native-pulse ansatz, we use non-gradient optimizers. Although gradients cannot be derived from shift-parameter rules like the gate ansatz, non-gradient optimizers will try to minimize the cost function using finite-difference approaches. Our methods of incrementally constructing the ansatz prevent non-gradient optimizers from failing to work with huge dimensions.

Simulators and NISQ machines are employed to examine our methods. On the simulators, we display an energy-distance curve for several molecules. The energy curves closely resemble those generated using the Full configuration interaction (FCI) approach. The results demonstrate that our pulse model may approximate the lowest energy states of molecules with a much shorter duration. Then, our programs are executed on NISQ machines. With PAN, we achieve greater performance than previous works. In addition, we demonstrate that tuning frequencies on NISQ computers are reasonable and feasible.

V. DESIGN AND IMPLEMENTATION DETAILS

A. Gate Ansatz versus Native-Pulse Ansatz

In the proposed PAN, we replace the basic element of the variational quantum circuit with a native pulse and stack quantum pulses to produce a native-pulse ansatz. The training process changes the parameters of the native pulses, thus obviating the requirement for decomposition into native gates and further transformation into pulses. To create a native-pulse ansatz, we must guarantee that the employed pulses are parametric pulses supported by the NISQ device. In the process, it is optional whether they correspond to a particular gate. Since we are employing native-pulse as building blocks for our ansatz, we need to explore all available parameters that can be tuned in the native pulse. The parameters of a gate-based ansatz are the angles of rotation gates. These gates will be decomposed into native gates before being implemented using microwave pulses and phase shifts. The microwave pulses are applied to qubits, while the phase shift is acting on classical electronics. When the angles for the rotation gates change, we observe changes in phase shift. However, the microwave pulses have not changed. Consequently, gate-based methods cannot take advantage of parametric pulses. So, we choose to directly adjust the parameters of the microwave pulses acting on qubits. In this way, we introduce possibilities to simplify the signals acting on pulses, thus reducing the

interaction between qubits and the environment. As shown in Figure 4, we are able to reduce the number of abstract layers.

Another advantage of adjusting pulse parameters instead of gate-angle is the mitigation of gate-to-pulse compilation noise. To experimentally realize a continuous parametric gate such as $RX(\pi/4)$, the amplitude of $X_{\pi/4}$ pulse will be set to be half of that of a $X_{\pi/2}$ pulse, i.e., $A_{\pi/4} = A_{\pi/2}/2$. However, this step introduces noise due to the nonlinearity in NISQ devices [31]. The pulse learning protocol directly tunes the underlying pulse parameter and avoids the unnecessary high-level compilation noise.

B. Parameters of Native-Pulse Ansatz

Tuning amplitudes. With native-pulse ansatz, we can tune parameters that are not accessible in gate-based ansatz. The amplitudes of the pulses on the drive and control channels, for example, are invisible to gate-level users. The unitary of a single-qubit native pulse (SNP) can be achieved by combining multiple native gates, albeit with a significantly longer latency. We use CR gate as a reference to generate our two-qubit native pulse (TNP), since the CR gate is the most basic element that can trigger the entanglement of two qubits. Both SNP and TNP are initialized with zeros as their amplitudes. The reason is explained in section V-D.

We can see from Eq. 5 and 4 that when we change the parameters of the pulses, it will affect the strength of the signal on the control channel of $d_i(t)$, which eventually affects the drive Hamiltonian. Experimental results presented in Table II confirm the advantages of pulse ansatz over gate ansatz. For experiments in Table II, the target is to solve the ground state energy of H_2 with VQE on the NISQ machine ibmq_jakarta. By comparing the results of SNP, TNP, TNP+SNP, and the two-gate ansatz, we demonstrate that the pulse ansatz provides a better energy value for the task in 31.2% less duration. The purpose of comparing the two-gate ansatz and the TNP+SNP pulse circuit is to highlight the advantages of native-pulse ansatz construction, as CX and TNP are the simplest 2-qubit operations on the gate-level and pulse-level, respectively.

Clifford and T gates are universal to perform arbitrary quantum operations [35], so gate calibrations mainly fine-tune a discrete set of $\pi/2$ and π pulses corresponding to Clifford operations [69]. In the progressive pulse learning protocol, pulse parameters are continuously varied, so it is necessary to verify that parametric pulses still produce physical quantum operations, i.e., pulses correspond to quantum operations and can be implemented with a high fidelity [77].

Tuning frequencies. We demonstrate the performance of pulse implementation by running a pulse version of the gate sequence $(CX + H + H^\dagger + CX^\dagger)$ under different frequency detuning. If the pulse block $(CX + H)$ is physically feasible to realize, when pulse detuning is zero, the circuit should produce a final $|00\rangle$ state with high probability. Experiment results in Figure 5 show a near-to-one prob $\langle 00 | \rho | 00 \rangle$ readout result for the zero detuning case and thus prove the feasibility of parametric pulse operations. The high-fidelity result also indicates that our

TABLE II
COMPARISON OF TRAINABILITY FOR DIFFERENT PULSE CIRCUITS AND GATE CIRCUITS ON IBMQ_JAKARTA.

Operations	Circuit Level	Molecule Bond Length	Reference Energy	VQE (H_2) Result	Duration(on ibmq_jakarta)
SNP	Pulse Circuit	0.1Å	2.710H	4.380H	71.1ns
TNP	Pulse Circuit	0.1Å	2.710H	2.927H	163.6ns
SNP	Pulse Circuit	0.75Å	-1.137H	-0.549H	71.1ns
TNP	Pulse Circuit	0.75Å	-1.137H	-1.032H	163.6ns
TNP + SNP	Pulse Circuit	0.75Å	-1.137H	-1.036H	234.7ns
Two Gate Ansatz	Gate Circuit	0.75Å	-1.137H	-0.534H	341.3ns

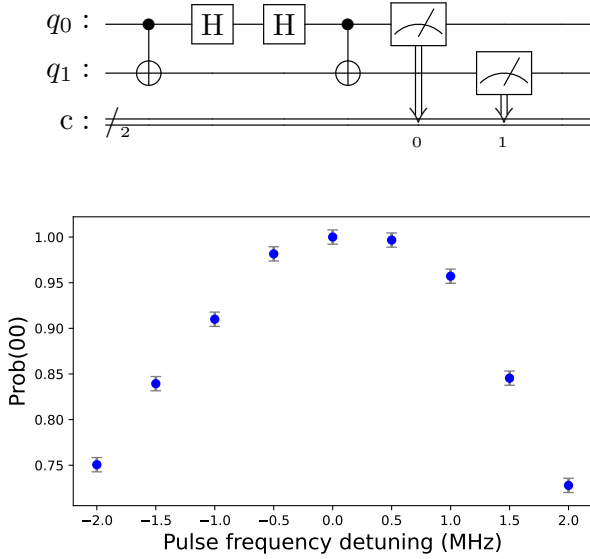


Fig. 5. Demonstrating the performance of pulse tuning. The circuit is realized through frequency-tuned pulse sequences. The probability of getting $|00\rangle$ state for the zero detuning indicates that parametric pulse operations are physically feasible and can be implemented with high fidelity. The change of final state under different detuning indicates that the variation of pulse parameter indeed physically changes the corresponding quantum operations. Note that here we apply the measurement error mitigation technique [30] which reduces the impact of readout errors.

pulse learning schedule will not introduce additional noise and can be authentically implemented.

In addition, the frequency detuned results verify that the magnitude of the detuning range we choose ($\approx MHz$) is wide enough such that the variation of pulse parameters can lead to the obvious change of the corresponding operation, and the resolution of pulse variation in the learning process is appropriate to ensure fast convergence and reduce the occurrence of the barren plateau.

C. Ansatz Construction

Variational quantum algorithms usually consist of parametric circuits with a fixed structure. The main focus in the current VQA research community is to address an efficient way to find the configuration of ansatzes. Traditional ways of finding ansatzes are mostly physics or chemistry inspired, which may

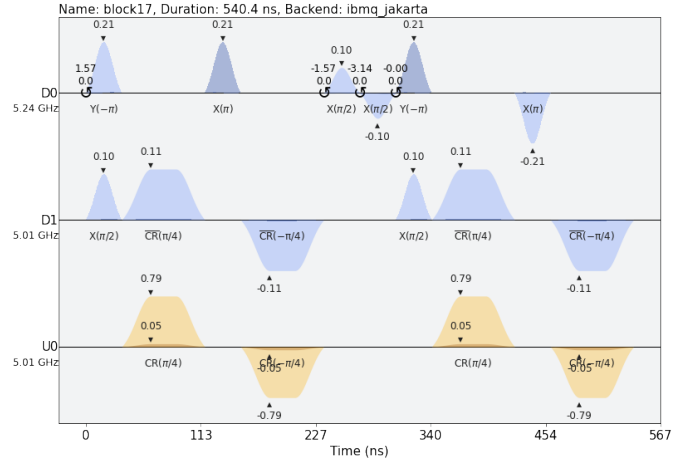


Fig. 6. Pulse schedules of “CX+H+H+CX” circuit. D0 and D1 are the drive channels on the first and the second qubits. They control the transmission from input signals to gate operations. U0 is the control channel which provides supplementary control over the qubit to the drive channel. These are often associated with multi-qubit gate operations [2]. The two qubit basis gate CNOT is realized through two $\pi/4$ cross-resonance pulses plus one $\pi/2$ X pulse. Single qubit gates are first XY decomposed and then implemented by XY pulses. [53]

be less intuitive and cost-inefficient. For instance, to achieve certain accuracy for algorithms utilizing time-evolving blocks such as QAOA, a few trotter steps may be sufficient [80], and a shallow circuit can realize it. However, the structured ansatzes are not adaptive, and it may be a great talent gone to waste when we aim to achieve a less demanding accuracy. Our progressive pulse learning protocol applies the aggregated instructions adaptively. The corresponding advantage is that the circuit depth is tailored for arbitrary desired accuracy and will not cause any experimental resource overhead. The next few sections illustrate the core steps in ansatz construction in detail.

D. Progressive Pulse Learning

Policy and Optimizer Selection. PAN supports the subsequent progressive learning by formulating policy. The first consideration in policy determination is to set the qubits of the entanglement with the topology map of the corresponding NISQ machine in order to achieve the effect of adaptive, i.e.,

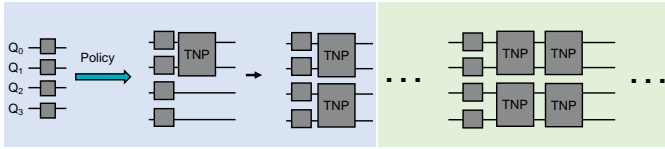


Fig. 7. Examples of a policy to grow the native-pulse ansatz. The policy includes TNP and SNP in different layers. TNP is responsible to guarantee the entanglement locally.

to save the consumption of qubits mapping. As shown in Figure 7, the policy for growing blocks is formulated. This policy starts with the SNPs on each qubit and is placed before the policy pulse circuits as a foundation for state preparation. The policy introduced TNP as the basic block, where TNP is the minimum basis pulse at which pulse level can implement the entanglement function. This policy ensures that the pulse circuit needs to consider the least number of parameters for training while completing entanglement. For the choice of non-gradient optimizer, we compared several candidates: Powell, COBYLA and Baysien Optimization. Powell is searched along the progressively generated conjugate direction, but Powell’s constraint creates some minor problems, Some function evaluations during the initial iteration may be outside the bounds if bounds are given, the initial guess is outside the bounds, and the parameter is full rank. And according to our observation, Bayesian optimization can fall into local points due to the effect of noise. Therefore, we finally choose COBYLA which completes the optimization by continuous linear approximation of the objective function and constraints by simplex construction of $n+1$ points in n dimensions.

Progressive Circuit Growing. In order to limit the number of parameters hold by the optimizer to ensure the efficiency of the optimizer, we propose a progressive approach to expand the pulse circuit. As shown in Figure 8, after the initial pulse circuit is trained, which is the first block. In the next steps, all the previously trained blocks are kept and fixed, and one new block is added for each step. In order to use the past experience, we also combine this block with all the previous blocks as the executed quantum program to the quantum computer. Such a structure allows for the combination of all the previously learned blocks at each layer, forming a hierarchy structure. Based on such a structure, our proposed framework naturally accumulates experience. In quantum computing, the quantum speed limit denotes the maximum rate of evolution of a quantum system, i.e., the limit of the minimum time for a quantum system to evolve between two distinguishable states [14], [60], [62]. Therefore, we may not be able to fully explore this part of Hilbert space in the first block of step growth, and it is reasonable to make the approaching target state with the subsequent steps in the progressive learning.

Pruning. We propose to further remove redundant parameters, i.e., redundant pulse, to achieve shorter duration, lower overhead, and lower noise. For PAN, firstly, some pulses containing amplitudes close to zero can be safely removed by trimming and fine-tuning. Second, the suboptimal nature of progressive

pulse learning leaves room for further optimization of the search circuit by reducing the number of gates.

As shown in Figure 8, specifically, we first train the searched pulse circuit from zero, collect all the amplitudes, and then remove the pulses where the amplitudes closest to zero are located. We ensure no degradation in the performance of the noise-free simulation compared to the unpruned pulse circuit. Thus, in NISQ machine experiments, the pruned pulse circuits show a small improvement in accuracy due to the reduction of a small number of noise sources.

VI. EVALUATION

A. Backend configuration

Our experiments are conducted both on simulator and NISQ machine. Simulator is used to validate that PAN considers the system model of quantum backends. Simulations are run on a server with two Intel Xeon E5-2630 CPUs (8 cores/CPU), 64 GB DRAM, with CentOS 7.4 as the operating system. To confirm that our framework works on NISQ machines, we conduct experiments on six IBM’s quantum systems: *ibm_cairo*, *ibmq_montreal*, *ibmq_toronto*, *ibmq_mumbai*, *ibmq_guadalupe* and *ibmq_jakarta*. And we chose VQE as our evaluation task, which consists of several molecules including H_2 , $HeH+$ and LiH . During the progressive learning process, each step contains up to 50 optimization iterations, and every quantum program is executed 1024 shots for sampling.

B. Native pulse

In the Table II, we compare the outcomes of different ansatz types for VQE tasks. The results are collected using NISQ machines. To determine the capabilities of our native-pulse model, we employ the simplest native-pulse model and compare its performance to that of native gates. The Table II demonstrates that our native-pulse approach can deliver superior VQE results in less durations. Pulse ansatz with only two native pulses can produce $-1.036H$ energy, whereas the two-gate ansatz can only achieve $-0.534H$ energy. The two-gate ansatz consists of both single-qubit and double-qubit gates as well. The duration of an ansatz is approximately 30% less than that of a gate ansatz. The duration numbers are calculated from the pulse schedules that produced by the same quantum backends. On simulator, we are able to produce superior VQE outcomes with significantly less latency.

C. Simulation results

To confirm that our framework can generate accurate energy curves for given molecules, we utilized simulators to evaluate our methodologies. The specifications of “fake” backends will be collected by the simulators and used as Hamiltonian configurations to execute the pulse simulation. The simulation results in Figure 9 and Figure 10 indicate that our methods can produce comparable outcomes to those of the full configuration interaction (FCI) methods. When attempting to compute the ground state energy of $HeH+$ molecules, we discovered that the simulated results are only 0.244% off from the FCI

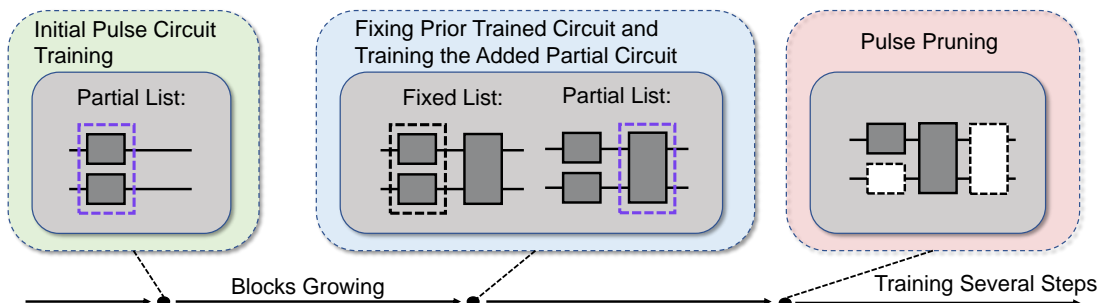


Fig. 8. During the training phase, we are able to determine which part of the parametric pulse is trained. The complete list of parameters comprises a fixed list and a “partial” list. The parameters in the fixed list will not be modified during the iteration. The parameters in the “partial” list will be modified instead. This is how pulse ansatz is constructed in order to maximize the flexibility of choosing different policies. We also apply naive pruning approaches during training to further simplify the pulse ansatz.

TABLE III
COMPARISON OF DURATION, PULSE COUNTS, AND ESTIMATED ENERGY OF GATE ANSATZES AND THE NATIVE-PULSE ANSATZ GENERATED BY PAN ON NISQ MACHINES.

Model	Ansatz Level	Qubits	Duration	Single-Qubit Pulse Count	Multi-Qubit Pulse Count	Molecule	Energy	Reference Energy
Random Genrated Ansatz	Gate Ansatz	2	682.7ns	16	2	H_2	-0.853	-1.137
RealAmplitude Ansatz [2]	Gate Ansatz	2	376.9ns	12	1	H_2	-0.974	-1.137
QuantumNAS [75]	Gate Ansatz	2	682.7ns	16	2	H_2	-1.033	-1.137
PAN	Pulse Ansatz	2	71.1ns	3	0	H_2	-1.100	-1.137
RealAmplitude Ansatz	Gate Ansatz	2	753.8ns	24	2	$HeH+$	-2.691	-2.863
PAN	Pulse Ansatz	2	199.1ns	1	1	$HeH+$	-2.866	-2.863
QuantumNAS	Gate Ansatz	6	7296.0ns	40	12	LiH	-6.914	-7.882
PAN	Pulse Ansatz	4	199.1ns	4	2	LiH	-7.590	-7.882

TABLE IV
RESULTS OF ESTIMATED ENERGY FOR MOLECULES IN DIFFERENT STEPS

Model	Cairo	Montreal	Toronto	NISQ machine Avg	Simulator	FCI	
H_2	Step I	-1.093 (3.870%)	-1.087 (4.398%)	-1.073 (5.629%)	-1.084 (4.661%)	-1.121 (1.407%)	-1.137
	Step II	-1.107 (2.639%)	-1.110 (2.375%)	-1.073 (5.629%)	-1.097 (3.518%)	-1.123 (1.231%)	-1.137
	Inaccuracy Reduction	31.83%	46.00%	0.000%	24.52%	12.51%	-
$HeH+$	Step I	-2.813 (1.746%)	-2.845 (0.663%)	-2.820 (1.485%)	-2.826 (1.292%)	-2.855 (0.279%)	-2.863
	Step II	-2.833 (1.047%)	-2.866 (0.105%)	-2.834 (1.013%)	-2.844 (0.664%)	-2.856 (0.244%)	-2.863
	Inaccuracy Reduction	40.03%	84.16%	31.78%	48.61%	12.54%	-

results. In the case of H_2 molecules, our simulated results deviate from FCI data by 1.23%. As shown in Table IV, the insertion of a native pulse in STEP two improved the performance of the native-pulse ansatz by approximately 12% on simulators. Overall, the simulation experiments verify our native-pulse ansatz approaches.

D. NISQ machine results

Our techniques are also evaluated on several NISQ computers. As presented in Figure 12 and Table III, a toy model of native-pulse ansatz is capable of producing promising results. In the instance of the $HeH+$ molecule, we may attain an average accuracy of 99.336%, with 99.895% being the highest

achievable accuracy. The absolute difference in energy is 0.003H. The accuracy is very close to the requirement of computational chemistry (0.0016H), which is the chemical accuracy constant for computational chemistry. It qualifies the typical minimum energy gap that can be verified through experiments. As for the H_2 molecule, we attain an average accuracy of 96.482% and a maximum accuracy of 97.625% using the same native-pulse ansatz. For LiH , a bigger molecule than those in the preceding cases, we may attain an energy accuracy of 96.295%. These accuracy figures are derived from NISQ machines with gate and measurement errors exceeding 1%. We observe that *ibmq_montreal* tends to return the best

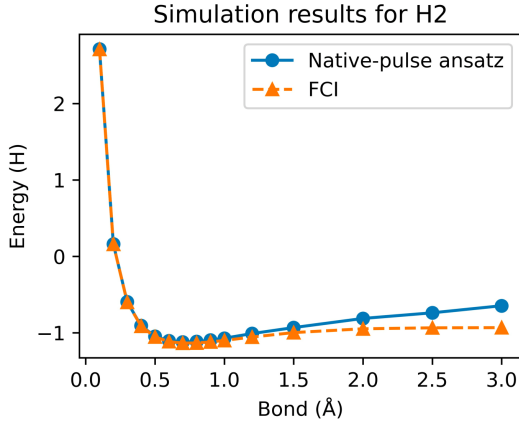


Fig. 9. Simulation result for H_2 molecule. The pulse ansatz curve mostly match the FCI value before Coulson-Fischer point [21]. The lowest energy point reaches accuracy of 97.69%

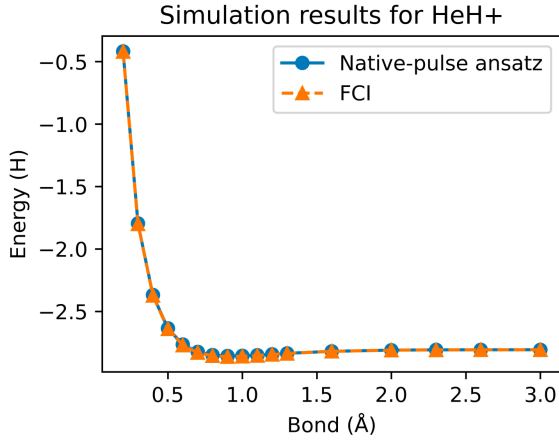


Fig. 10. Simulation result of HeH^+ molecule. The pulse ansatz curve almost match the FCI value for all shown bond length. The lowest energy point reaches accuracy of 99.756%

results, while *ibmq_mumbai* typically returns worse results. Then, we confirm that *ibmq_mumbai* has greater error rates for gates and measurements on average than *ibmq_montreal*.

The results collected from NISQ computers demonstrate that our approaches are highly error-tolerant. In terms of total duration time, our native-pulse approaches have significant advantages over the current gate ansatz generator. To ensure equality, the gate ansatz of the baselines is implemented on the same NISQ computer, and their duration is determined using the acquired pulse schedules. We are able to demonstrate a 97.3% reduction in ansatz duration compared to QuantumNAS, and our energy values for LiH are lower. With a duration decrease of 89.6%, our native-pulse method can obtain greater energy values while dealing with H_2 molecules. QuantumNAS does not report the energy numbers for the HeH^+ molecule. Thus we compare our techniques to the Real Amplitude Ansatz, which shows that we are able to reduce duration by 73.6% while maintaining ansatz performance.

Figure 11 depicts the relationships between the computed

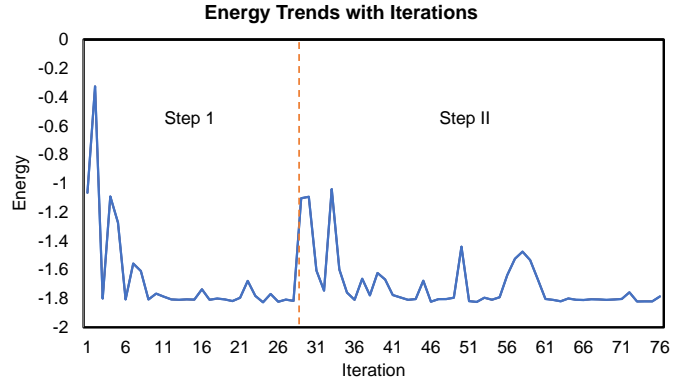


Fig. 11. Energy convergence with #iterations for a H_2 VQE task and the vertical dotted line in the middle separates the steps in progressive learning. The data is collected from *ibmq_montreal*. We can see several “peaks” on the curves. Because we are using non-gradient optimizer, possibilities are that attempts are made in a bad direction.

energy and the number of iterations. Despite the fact that it is not visible in Figure 11, we validate that our progressive approaches do work on VQE tasks. Since a non-gradient optimizer is deployed, we can observe several peaks of the curve where the non-gradient optimizer attempts to update the pulse ansatz’s parameters but obtains poorer results. As indicated in the Table IV, we are able to reduce the deviation from FCI values by around 40%, when native-pulses “grow” progressively. Only in one instance where the pulse ansatz were conducted on *ibmq_toronto* were the results not improved. Taking into account this failure, we find a 24% improvement for H_2 molecule experiments and a 48% improvement for HeH^+ molecule experiments.

E. Tuning frequencies

In Fig. IV, we detune the pulse frequency and use a few steps to estimate the energy of the H_2 molecule. The experimental results show that as we vary the detuning, the energy estimation scan over a broad range, which ensures that the pulse parameter variation in the learning step is wide enough to cover the ground energy. Moreover, the evident response of energy estimation with pulse parameterization shows that our ansatz structures are valid in covering all spin-orbital configurations of the electronic structure. The estimated energy can then progressively approach the desired ground energy through pulse parameters learning.

VII. RELATED WORK

Pulse Learning Approach: Ctrl-VQE [54] changes the pulse shape to perform state preparation. The methods are evaluated with Qutip [42] pulse simulator. And the results demonstrate that the coherence time required for state preparation is greatly reduced. VQP [49] uses pulses as basic components to build the QNN ansatz and exhibits latency advantages over gate-based QNN on a two-class image classification task. The experiments are mostly on Qiskit [52] pulse simulator. VQOC [25] presents a mathematical formalism of

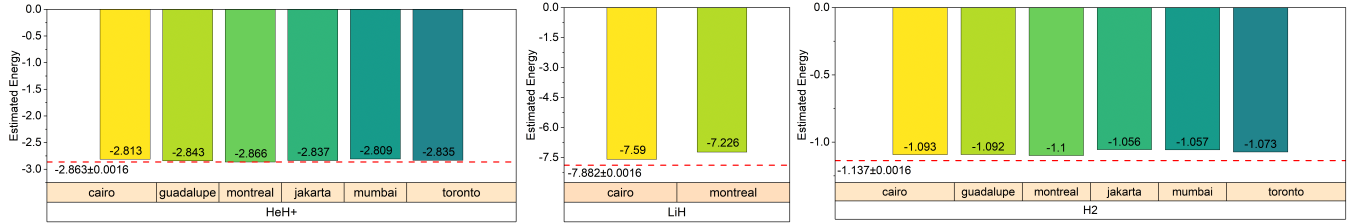


Fig. 12. Evaluation of native-pulse ansatz on NISQ machines for H_2 , HeH^+ , and LiH VQE tasks. NISQ machines includes *ibm_cairo*, *ibmq_montreal*, *ibmq_toronto*, *ibmq_mumbai*, *ibmq_guadalupe*, and *ibmq_jakarta*. Our toy ansatz are able to achieve great accuracy on all the NISQ machines. For *ibmq_montreal* where we obtain the best results, the average CNOT error is 1.518% as the average readout error is 3.457%. PAN is proven to be robust and error-resilient on NISQ machines.

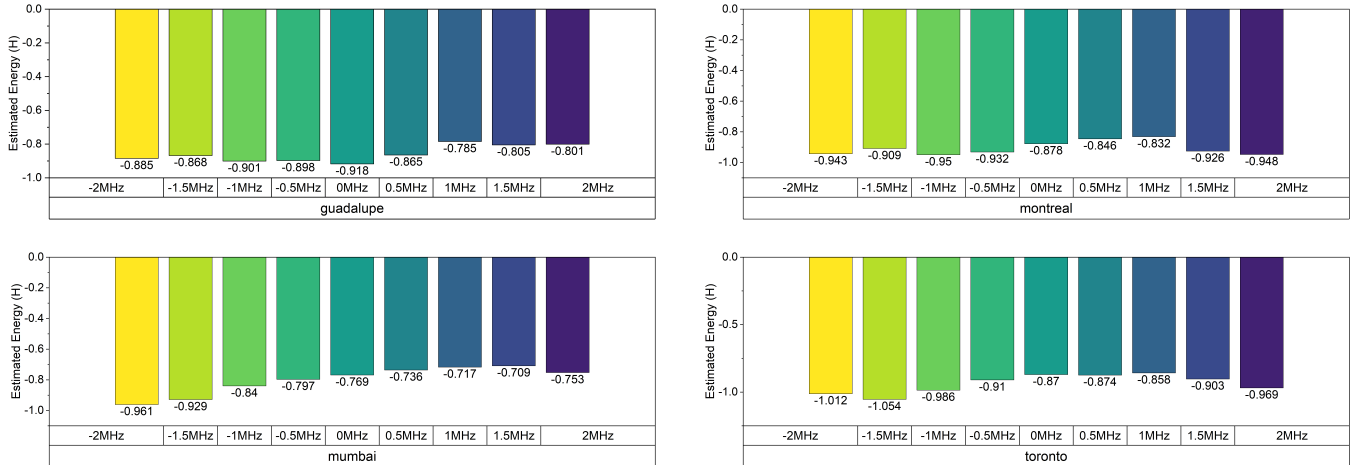


Fig. 13. Influence of frequency shift on the estimated energy. Even with a narrow frequency shift range, we notice obvious changes in the estimated energy. The experiments are conducted before convergence, the energy values are calculated for H_2 molecule. The experimental results show that as we vary the detuning frequency, the energy estimation scans over a broad range, which validates our methods to tune frequency in pulses.

optimal control, which acts on pulse optimization for VQA tasks. Their method is similar to Ctrl-VQE [54], but they take advantages of neutral atom’s properties. The evaluations are also performed on simulator. These previous works are exploratory and rely on classical simulations of small quantum systems [19], [25], [49], [54]. PAN, on the other hand, provides results from NISQ machines.

Ansatz Architecture Search: Hamiltonian simulation plays an important role in simulating quantum systems [43], [43], [59], [70]. Variational quantum algorithms can be deployed to perform Hamiltonian simulation. And previous works [43] pointed out that the choice of ansatz is important for VQAs. The conventional approaches of choosing ansatz depends heavily on the applications. [10], [57], [59] are specially designed for VQE tasks. The unitary coupled-cluster singles and doubles schele (UCCSD) is still the golden standards for VQE ansatz. UCCSD approximates the states of the molecule and can be implemented with qubits. QAS [28] proposes a noise-aware scheme to search for ansatz structure. The robustness to noise is demonstrated on simulators. QuantumNAS [75] presents a comprehensive framework for noise-adaptive co-search of the ansatz. Hardware topology is considered during the search algorithm. QuantumNAS validates

their methods with evaluations on NISQ machines.

Pulse Gate Compilation: [34] proposes a new compilation paradigm, based on the OpenPulse interface for IBM quantum computers. This work achieves lower error rates and shorter execution times in comparison with traditional gate-based compilation methods. Their technique is bootstrapped from existing gate calibrations, thus their pulses are in a simple form. [64] designs a general quantum compilation method to integrate multiple operations into larger units and then achieve high efficiency by optimizing this aggregate and creating corresponding custom control pulses.

VIII. CONCLUSION

PAN is a framework of constructing native-pulse ansatz for variational quantum algorithms. As a result of removing an abstraction layer of native gates, native pulses provide huge latency advantages. Then, we employ progressive learning to “expand” our ansatz. Thus, our pulse ansatz is better able to explore the Hilbert space, while the optimizer is still able to handle the problem. Extensive experiments are conducted on NISQ machines, and the results indicate that an average of 86% reduction in latency is obtained with up to 99.895% accuracy on small molecule VQE task.

REFERENCES

- [1] “IBM unveils breakthrough 127-qubit quantum processor,” <https://newsroom.ibm.com/2021-11-16-IBM-Unveils-Breakthrough-127-Qubit-Quantum-Processor>.
- [2] “Qiskit,” <https://qiskit.org/>.
- [3] A. Abbas, D. Sutter, C. Zoufal, A. Lucchi, A. Figalli, and S. Woerner, “The power of quantum neural networks,” *Nature Computational Science*, vol. 1, no. 6, pp. 403–409, 2021.
- [4] D. Aharonov and M. Ben-Or, “Fault-tolerant quantum computation with constant error rate,” *SIAM Journal on Computing*, 2008.
- [5] M. Ahsan, S. A. Z. Naqvi, and H. Anwer, “Quantum circuit engineering for correcting coherent noise,” *Physical Review A*, vol. 105, no. 2, p. 022428, 2022.
- [6] T. Alexander, N. Kanazawa, D. J. Egger, L. Capelluto, C. J. Wood, A. Javadi-Abhari, and D. C. McKay, “Qiskit pulse: Programming quantum computers through the cloud with pulses,” *Quantum Science and Technology*, vol. 5, no. 4, p. 044006, 2020.
- [7] H. Alghassi, A. Deshmukh, N. Ibrahim, N. Robles, S. Woerner, and C. Zoufal, “A variational quantum algorithm for the feynman-kac formula,” *Quantum*, vol. 6, p. 730, 2022.
- [8] F. Arute, K. Arya, R. Babbush, D. Bacon, J. C. Bardin, R. Barends, R. Biswas, S. Boixo, F. G. Brandao, D. A. Buell et al., “Quantum supremacy using a programmable superconducting processor,” *Nature*, vol. 574, no. 7779, pp. 505–510, 2019.
- [9] S. Axelrod, E. Shakhnovich, and R. Gómez-Bombarelli, “Excited state non-adiabatic dynamics of large photoswitchable molecules using a chemically transferable machine learning potential,” *Nature communications*, vol. 13, no. 1, pp. 1–11, 2022.
- [10] R. J. Bartlett and M. Musiał, “Coupled-cluster theory in quantum chemistry,” *Reviews of Modern Physics*, vol. 79, no. 1, p. 291, 2007.
- [11] J. Biamonte, P. Wittek, N. Pancotti, P. Rebentrost, N. Wiebe, and S. Lloyd, “Quantum machine learning,” *Nature*, vol. 549, no. 7671, pp. 195–202, 2017.
- [12] S. Boixo, S. V. Isakov, V. N. Smelyanskiy, R. Babbush, N. Ding, Z. Jiang, M. J. Bremner, J. M. Martinis, and H. Neven, “Characterizing quantum supremacy in near-term devices,” *Nature Physics*, vol. 14, no. 6, pp. 595–600, 2018.
- [13] C. D. Bruzewicz, J. Chiaverini, R. McConnell, and J. M. Sage, “Trapped-ion quantum computing: Progress and challenges,” *Applied Physics Reviews*, vol. 6, no. 2, p. 021314, 2019.
- [14] D. Burgarth, J. Borggaard, and Z. Zimborás, “Quantum distance to uncontrollability and quantum speed limits,” *Physical Review A*, vol. 105, no. 4, p. 042402, 2022.
- [15] T. Caneva, T. Calarco, and S. Montangero, “Chopped random-basis quantum optimization,” *Physical Review A*, vol. 84, no. 2, p. 022326, 2011.
- [16] Y. Cao, J. Romero, J. P. Olson, M. Degroote, P. D. Johnson, M. Kieferová, I. D. Kivlichan, T. Menke, B. Peropadre, N. P. Sawaya et al., “Quantum chemistry in the age of quantum computing,” *Chemical reviews*, vol. 119, no. 19, pp. 10856–10915, 2019.
- [17] M. Cerezo, A. Arrasmith, R. Babbush, S. C. Benjamin, S. Endo, K. Fujii, J. R. McClean, K. Mitarai, X. Yuan, L. Cincio et al., “Variational quantum algorithms,” *Nature Reviews Physics*, vol. 3, no. 9, pp. 625–644, 2021.
- [18] J. Cheng, H. Deng, and X. Qia, “Accqoc: Accelerating quantum optimal control based pulse generation,” in *2020 ACM/IEEE 47th Annual International Symposium on Computer Architecture (ISCA)*. IEEE, 2020, pp. 543–555.
- [19] A. Choquette, A. Di Paolo, P. K. Barkoutsos, D. Sénéchal, I. Tavernelli, and A. Blais, “Quantum-optimal-control-inspired ansatz for variational quantum algorithms,” *Physical Review Research*, vol. 3, no. 2, p. 023092, 2021.
- [20] J. Clarke and F. K. Wilhelm, “Superconducting quantum bits,” *Nature*, vol. 453, no. 7198, pp. 1031–1042, 2008.
- [21] C. A. Coulson and I. Fischer, “Xxxiv. notes on the molecular orbital treatment of the hydrogen molecule,” *The London, Edinburgh, and Dublin Philosophical Magazine and Journal of Science*, vol. 40, no. 303, pp. 386–393, 1949.
- [22] P. Das, A. Locharla, and C. Jones, “Lilliput: a lightweight low-latency lookup-table decoder for near-term quantum error correction,” in *Proceedings of the 27th ACM International Conference on Architectural Support for Programming Languages and Operating Systems*, 2022, pp. 541–553.
- [23] P. Das, C. A. Pattison, S. Manne, D. M. Carmean, K. M. Svore, M. Qureshi, and N. Delfosse, “Afs: Accurate, fast, and scalable error-decoding for fault-tolerant quantum computers,” in *2022 IEEE International Symposium on High-Performance Computer Architecture (HPCA)*. IEEE, 2022, pp. 259–273.
- [24] P. de Fouquieres, S. G. Schirmer, S. J. Glaser, and I. Kuprov, “Second order gradient ascent pulse engineering,” *Journal of Magnetic Resonance*, vol. 212, no. 2, pp. 412–417, 2011.
- [25] R. de Keijzer, O. Tse, and S. Kokkelmans, “Pulse based variational quantum optimal control for hybrid quantum computing,” *arXiv preprint arXiv:2202.08908*, 2022.
- [26] Y. Ding and F. T. Chong, “Quantum computer systems: Research for noisy intermediate-scale quantum computers,” *Synthesis Lectures on Computer Architecture*, vol. 15, no. 2, pp. 1–227, 2020.
- [27] Y. Ding, P. Gokhale, S. F. Lin, R. Rines, T. Propson, and F. T. Chong, “Systematic crosstalk mitigation for superconducting qubits via frequency-aware compilation,” in *2020 53rd Annual IEEE/ACM International Symposium on Microarchitecture (MICRO)*. IEEE, 2020, pp. 201–214.
- [28] Y. Du, T. Huang, S. You, M.-H. Hsieh, and D. Tao, “Quantum circuit architecture search for variational quantum algorithms,” *npj Quantum Information*, vol. 8, no. 1, pp. 1–8, 2022.
- [29] E. Farhi, J. Goldstone, and S. Gutmann, “A quantum approximate optimization algorithm,” *arXiv preprint arXiv:1411.4028*, 2014.
- [30] L. Funcke, T. Hartung, K. Jansen, S. Kühn, P. Stornati, and X. Wang, “Measurement error mitigation in quantum computers through classical bit-flip correction,” 2020. [Online]. Available: <https://arxiv.org/abs/2007.03663>
- [31] J. Gil-Lopez, M. Santandrea, G. Roland, B. Brecht, C. Eigner, R. Ricken, V. Quiring, and C. Silberhorn, “Improved non-linear devices for quantum applications,” *New Journal of Physics*, vol. 23, no. 6, p. 063082, jun 2021. [Online]. Available: <https://doi.org/10.1088%2F1367-2630%2F2021063082>
- [32] P. Gokhale, O. Angiuli, Y. Ding, K. Gui, T. Tomesh, M. Suchara, M. Martonosi, and F. T. Chong, “Optimization of simultaneous measurement for variational quantum eigensolver applications,” in *2020 IEEE International Conference on Quantum Computing and Engineering (QCE)*. IEEE, 2020, pp. 379–390.
- [33] P. Gokhale, Y. Ding, T. Propson, C. Winkler, N. Leung, Y. Shi, D. I. Schuster, H. Hoffmann, and F. T. Chong, “Partial compilation of variational algorithms for noisy intermediate-scale quantum machines,” in *Proceedings of the 52nd Annual IEEE/ACM International Symposium on Microarchitecture*, 2019, pp. 266–278.
- [34] P. Gokhale, A. Javadi-Abhari, N. Earnest, Y. Shi, and F. T. Chong, “Optimized quantum compilation for near-term algorithms with open-pulse,” in *2020 53rd Annual IEEE/ACM International Symposium on Microarchitecture (MICRO)*. IEEE, 2020, pp. 186–200.
- [35] D. Gottesman, “Theory of fault-tolerant quantum computation,” *Phys. Rev. A*, vol. 57, pp. 127–137, Jan 1998. [Online]. Available: <https://link.aps.org/doi/10.1103/PhysRevA.57.127>
- [36] R. Grimm, M. Weidemüller, and Y. B. Ovchinnikov, “Optical dipole traps for neutral atoms,” in *Advances in atomic, molecular, and optical physics*. Elsevier, 2000, vol. 42, pp. 95–170.
- [37] L. K. Grover, “A fast quantum mechanical algorithm for database search,” in *Proceedings of the twenty-eighth annual ACM symposium on Theory of computing*, 1996, pp. 212–219.
- [38] G. G. Guerreschi and A. Y. Matsuura, “Qaoa for max-cut requires hundreds of qubits for quantum speed-up,” *Scientific reports*, vol. 9, no. 1, pp. 1–7, 2019.
- [39] J. Herrmann, S. M. Lima, A. Remm, P. Zapletal, N. A. McMahon, C. Scarato, F. Swiadek, C. K. Andersen, C. Hellings, S. Krinner et al., “Realizing quantum convolutional neural networks on a superconducting quantum processor to recognize quantum phases,” *Nature Communications*, vol. 13, no. 1, pp. 1–7, 2022.
- [40] F. Hua, Y. Chen, Y. Jin, C. Zhang, A. Hayes, Y. Zhang, and E. Z. Zhang, “Autobraid: A framework for enabling efficient surface code communication in quantum computing,” in *MICRO-54: 54th Annual IEEE/ACM International Symposium on Microarchitecture*, 2021, pp. 925–936.
- [41] H.-Y. Huang, M. Broughton, J. Cotler, S. Chen, J. Li, M. Mohseni, H. Neven, R. Babbush, R. Kueng, J. Preskill et al., “Quantum advantage in learning from experiments,” *Science*, vol. 376, no. 6598, pp. 1182–1186, 2022.

- [42] J. R. Johansson, P. D. Nation, and F. Nori, “Qutip: An open-source python framework for the dynamics of open quantum systems,” *Computer Physics Communications*, vol. 183, no. 8, pp. 1760–1772, 2012.
- [43] A. Kandala, A. Mezzacapo, K. Temme, M. Takita, M. Brink, J. M. Chow, and J. M. Gambetta, “Hardware-efficient variational quantum eigensolver for small molecules and quantum magnets,” *Nature*, vol. 549, no. 7671, pp. 242–246, 2017.
- [44] J. Kelly, R. Barends, A. G. Fowler, A. Megrant, E. Jeffrey, T. C. White, D. Sank, J. Y. Mutus, B. Campbell, Y. Chen et al., “State preservation by repetitive error detection in a superconducting quantum circuit,” *Nature*, vol. 519, no. 7541, pp. 66–69, 2015.
- [45] P. Kok, W. J. Munro, K. Nemoto, T. C. Ralph, J. P. Dowling, and G. J. Milburn, “Linear optical quantum computing with photonic qubits,” *Reviews of modern physics*, vol. 79, no. 1, p. 135, 2007.
- [46] N. Leung, M. Abdelhafez, J. Koch, and D. Schuster, “Speedup for quantum optimal control from automatic differentiation based on graphics processing units,” *Physical Review A*, vol. 95, no. 4, p. 042318, 2017.
- [47] G. Li, Y. Shi, and A. Javadi-Abhari, “Software-hardware co-optimization for computational chemistry on superconducting quantum processors,” in *2021 ACM/IEEE 48th Annual International Symposium on Computer Architecture (ISCA)*. IEEE, 2021, pp. 832–845.
- [48] G. Li, A. Wu, Y. Shi, A. Javadi-Abhari, Y. Ding, and Y. Xie, “Paulihedral: a generalized block-wise compiler optimization framework for quantum simulation kernels,” in *Proceedings of the 27th ACM International Conference on Architectural Support for Programming Languages and Operating Systems*, 2022, pp. 554–569.
- [49] Z. Liang, H. Wang, J. Cheng, Y. Ding, H. Ren, X. Qian, S. Han, W. Jiang, and Y. Shi, “Variational quantum pulse learning,” *arXiv preprint arXiv:2203.17267*, 2022.
- [50] J.-G. Liu, Y.-H. Zhang, Y. Wan, and L. Wang, “Variational quantum eigensolver with fewer qubits,” *Physical Review Research*, vol. 1, no. 2, p. 023025, 2019.
- [51] M. Lubasch, J. Joo, P. Moinier, M. Kiffner, and D. Jaksch, “Variational quantum algorithms for nonlinear problems,” *Physical Review A*, vol. 101, no. 1, p. 010301, 2020.
- [52] D. C. McKay, T. Alexander, L. Bello, M. J. Biercuk, L. Bishop, J. Chen, J. M. Chow, A. D. Córcoles, D. Egger, S. Filipp et al., “Qiskit backend specifications for openqasm and openpulse experiments,” *arXiv preprint arXiv:1809.03452*, 2018.
- [53] D. C. McKay, C. J. Wood, S. Sheldon, J. M. Chow, and J. M. Gambetta, “Efficient z gates for quantum computing,” *Phys. Rev. A*, vol. 96, p. 022330, Aug 2017. [Online]. Available: <https://link.aps.org/doi/10.1103/PhysRevA.96.022330>
- [54] O. R. Meitei, B. T. Gard, G. S. Barron, D. P. Pappas, S. E. Economou, E. Barnes, and N. J. Mayhall, “Gate-free state preparation for fast variational quantum eigensolver simulations,” *npj Quantum Information*, vol. 7, no. 1, pp. 1–11, 2021.
- [55] N. Moll, P. Barkoutsos, L. S. Bishop, J. M. Chow, A. Cross, D. J. Egger, S. Filipp, A. Fuhrer, J. M. Gambetta, M. Ganzhorn et al., “Quantum optimization using variational algorithms on near-term quantum devices,” *Quantum Science and Technology*, vol. 3, no. 3, p. 030503, 2018.
- [56] P. Neumann, N. Mizuochi, F. Rempp, P. Hemmer, H. Watanabe, S. Yamasaki, V. Jacques, T. Gaebel, F. Jelezko, and J. Wrachtrup, “Multipartite entanglement among single spins in diamond,” *science*, vol. 320, no. 5881, pp. 1326–1329, 2008.
- [57] P. J. O’Malley, R. Babbush, I. D. Kivlichan, J. Romero, J. R. McClean, R. Barends, J. Kelly, P. Roushan, A. Tranter, N. Ding et al., “Scalable quantum simulation of molecular energies,” *Physical Review X*, vol. 6, no. 3, p. 031007, 2016.
- [58] W. Paul, “Electromagnetic traps for charged and neutral particles,” *Reviews of modern physics*, vol. 62, no. 3, p. 531, 1990.
- [59] A. Peruzzo, J. McClean, P. Shadbolt, M.-H. Yung, X.-Q. Zhou, P. J. Love, A. Aspuru-Guzik, and J. L. O’Brien, “A variational eigenvalue solver on a photonic quantum processor,” *Nature communications*, vol. 5, no. 1, pp. 1–7, 2014.
- [60] D. P. Pires, M. Cianciaruso, L. C. Céleri, G. Adesso, and D. O. Soares-Pinto, “Generalized geometric quantum speed limits,” *Physical Review X*, vol. 6, no. 2, p. 021031, 2016.
- [61] A. P. Place, L. V. Rodgers, P. Mundada, B. M. Smitham, M. Fitzpatrick, Z. Leng, A. Premkumar, J. Bryon, A. Vrajitoarea, S. Sussman et al., “New material platform for superconducting transmon qubits with coherence times exceeding 0.3 milliseconds,” *Nature communications*, vol. 12, no. 1, pp. 1–6, 2021.
- [62] P. M. Poggi, S. Campbell, and S. Deffner, “Diverging quantum speed limits: a herald of classicality,” *PRX Quantum*, vol. 2, no. 4, p. 040349, 2021.
- [63] K. Sharma, M. Cerezo, L. Cincio, and P. J. Coles, “Trainability of dissipative perceptron-based quantum neural networks,” *Physical Review Letters*, vol. 128, no. 18, p. 180505, 2022.
- [64] Y. Shi, N. Leung, P. Gokhale, Z. Rossi, D. I. Schuster, H. Hoffmann, and F. T. Chong, “Optimized compilation of aggregated instructions for realistic quantum computers,” in *Proceedings of the Twenty-Fourth International Conference on Architectural Support for Programming Languages and Operating Systems*, 2019, pp. 1031–1044.
- [65] P. W. Shor, “Polynomial-time algorithms for prime factorization and discrete logarithms on a quantum computer,” *SIAM review*, vol. 41, no. 2, pp. 303–332, 1999.
- [66] S. Stein, N. Wiebe, Y. Ding, P. Bo, K. Kowalski, N. Baker, J. Ang, and A. Li, “Eqc: ensembled quantum computing for variational quantum algorithms,” in *Proceedings of the 49th Annual International Symposium on Computer Architecture*, 2022, pp. 59–71.
- [67] H. L. Tang, V. Shkolnikov, G. S. Barron, H. R. Grimsley, N. J. Mayhall, E. Barnes, and S. E. Economou, “qubit-adapt-vqe: An adaptive algorithm for constructing hardware-efficient ansätze on a quantum processor,” *PRX Quantum*, vol. 2, no. 2, p. 020310, 2021.
- [68] S. Tannu, P. Das, R. Ayanzadeh, and M. Qureshi, “Hammer: boosting fidelity of noisy quantum circuits by exploiting hamming behavior of erroneous outcomes,” in *Proceedings of the 27th ACM International Conference on Architectural Support for Programming Languages and Operating Systems*, 2022, pp. 529–540.
- [69] L. S. Theis, F. Motzoi, S. Machnes, and F. K. Wilhelm, “Counteracting systems of diabaticities using DRAG controls: The status after 10 years,” *EPL (Europhysics Letters)*, vol. 123, no. 6, p. 60001, oct 2018. [Online]. Available: <https://doi.org/10.1209/2F0295-5075%2F123%2F60001>
- [70] J. Tilly, H. Chen, S. Cao, D. Picozzi, K. Setia, Y. Li, E. Grant, L. Wossnig, I. Rungger, G. H. Booth et al., “The variational quantum eigensolver: a review of methods and best practices,” *arXiv preprint arXiv:2111.05176*, 2021.
- [71] T. Tomesh, P. Gokhale, V. Omole, G. S. Ravi, K. N. Smith, J. Vizlai, X.-C. Wu, N. Hardavellas, M. R. Martonosi, and F. T. Chong, “Supermarq: A scalable quantum benchmark suite,” in *2022 IEEE International Symposium on High-Performance Computer Architecture (HPCA)*. IEEE, 2022, pp. 587–603.
- [72] T. Tomesh, K. Gui, P. Gokhale, Y. Shi, F. T. Chong, M. Martonosi, and M. Suchara, “Optimized quantum program execution ordering to mitigate errors in simulations of quantum systems,” in *2021 International Conference on Rebooting Computing (ICRC)*. IEEE, 2021, pp. 1–13.
- [73] L. M. Vandersypen, M. Steffen, G. Breyta, C. S. Yannoni, M. H. Sherwood, and I. L. Chuang, “Experimental realization of shor’s quantum factoring algorithm using nuclear magnetic resonance,” *Nature*, vol. 414, no. 6866, pp. 883–887, 2001.
- [74] D. Wang, O. Higgott, and S. Brierley, “Accelerated variational quantum eigensolver,” *Physical review letters*, vol. 122, no. 14, p. 140504, 2019.
- [75] H. Wang, Y. Ding, J. Gu, Y. Lin, D. Z. Pan, F. T. Chong, and S. Han, “Quantumnas: Noise-adaptive search for robust quantum circuits,” in *2022 IEEE International Symposium on High-Performance Computer Architecture (HPCA)*. IEEE, 2022, pp. 692–708.
- [76] S. Wang, E. Fontana, M. Cerezo, K. Sharma, A. Sone, L. Cincio, and P. J. Coles, “Noise-induced barren plateaus in variational quantum algorithms,” *Nature communications*, vol. 12, no. 1, pp. 1–11, 2021.
- [77] C. Weedbrook, S. Pirandola, R. García-Patrón, N. J. Cerf, T. C. Ralph, J. H. Shapiro, and S. Lloyd, “Gaussian quantum information,” *Rev. Mod. Phys.*, vol. 84, pp. 621–669, May 2012. [Online]. Available: <https://link.aps.org/doi/10.1103/RevModPhys.84.621>
- [78] J. Werschnik and E. Gross, “Quantum optimal control theory,” *Journal of Physics B: Atomic, Molecular and Optical Physics*, vol. 40, no. 18, p. R175, 2007.
- [79] S. L. Wu and S. Yoo, “Challenges and opportunities in quantum machine learning for high-energy physics,” *Nature Reviews Physics*, vol. 4, no. 3, pp. 143–144, 2022.
- [80] X. Yang, X. Nie, Y. Ji, T. Xin, D. Lu, and J. Li, “Improved quantum computing with the higher-order trotter decomposition,” 2022. [Online]. Available: <https://arxiv.org/abs/2205.02520>